TÜBİTAK

Turkish Journal of Chemistry

http://journals.tubitak.gov.tr/chem/

Research Article

Turk J Chem
(2016) 40: 1044 – 1054

doi:10.3906/kim-1606-4

Biosorption potential of surface-modified waste sugar beet pulp for the removal of Reactive Yellow 2 (RY2) anionic dye

Sibel TUNALI AKAR[1,*], Sema ÇELİK[2], Dilek TUNÇ[2], Yasemin YETİMOĞLU BALK[2], Tamer AKAR[1]

[1]Department of Chemistry, Faculty of Arts and Science, Eskişehir Osmangazi University, Eskişehir, Turkey
[2]Department of Chemistry, Graduate School of Natural and Applied Sciences, Eskişehir Osmangazi University, Eskişehir, Turkey

Received: 03.06.2016 • **Accepted/Published Online:** 04.11.2016 • **Final Version:** 22.12.2016

Abstract: Tetra–n-butylammonium bromide modified sugar beet pulp (TBAB–SBP) with good biosorption and regeneration potential was prepared for removal of dye from contaminated solutions. The decolorization performance of TBAB–SBP was investigated using Reactive Yellow 2 (RY2) as a model dye. The characterization of the modified biosorbent was investigated by IR, SEM, zeta potential, and BET surface area analysis to discuss the decolorization mechanism. The effects of initial pH, biosorbent amount, contact time, dye concentration, and flow rate on the treatment process were examined. The experimental kinetic data were well predicted by the pseudo-second-order kinetic model and Langmuir isotherm with a maximum monolayer biosorption capacity up to 7.20×10^{-5} mol g^{-1}. The modified biosorbent was also successfully used in dynamic flow treatment mode. Moreover, the prepared biosorbent could be regenerated using 0.01 M NaOH during 15 biosorption/desorption cycles. Experimental results indicated that the electrostatic interaction, complexation, and ion exchange were possible interactions in the decolorization process. The real wastewater treatment application showed that TBAB–SBP is a suitable green-type biosorbent for the decolorization of reactive dye-contaminated aquatic media.

Key words: Decolorization, surface modification, kinetics, isotherms, real wastewater

1. Introduction

Dyes are complex organic chemicals and different kinds of synthetic dyes are used for the products of several industries including textile, paper, printing, plastic, etc. These industries generally consume substantial volumes of water and produce dye-contaminated effluents. Treatment of the colored effluents is an important issue because of their toxic and mutagenic effects on life and serious ecological damage.[1,2]

Sludge formation at the end of the processes and high application cost are significant technical problems of the conventional treatment process such as coagulation, flocculation, membrane filtration, and irradiation. Although certain microbial enzymes can degrade dye molecules, the possible production of toxic amine compounds as a result of the cleavage of diazo bonds is a significant drawback of the biodegradation process.[3] In this context, biosorption has attracted interest as a valuable technology in the field of water treatment and based on the possible interactions between pollutant and the cellular surface of the biomaterial. Functional groups on the biomass surface like hydroxyl, carboxyl, sulfhydryl, amino, phosphoryl, and thiol are potential

*Correspondence: stunali@ogu.edu.tr

binding sites for removal of organic or inorganic pollutants. One or more mechanisms such as physical adsorption, microprecipitation, surface complexation, and ion exchange can play a role in the biosorptive treatment process.[4]

Among various types of biosorbent materials, lignocellulosic biomasses as industrial wastes have been more convenient in biosorption applications with the advantages of good sorption performance, physical and chemical characteristics, and low or no costs. Lignin, cellulose, and hemicellulose are structural components of these biomaterials and provide potential binding sites for pollutants.[5,6] *Punica granatum* L. peels,[7] cocoa pod husk,[8] *Capsicum annum* seeds,[9] rice husk,[10] pineapple leaf,[11] sugarcane bagasse,[12] *Phaseolus vulgaris* L.,[13] and olive mill solid residue[14] are some examples of recent reports related to agricultural origin biosorbent materials. In addition to efforts related to preparation of the green-type biosorbent materials, surface modifications by different agents have been suggested for the improvement of the sorption potential of biomaterials.[6,15,16]

In the present study, modified biosorbent was prepared from waste biomass of the sugar production process. The natural form of sugar beet pulp biomass was previously used for the removal of synthetic dye and heavy metal contaminants such as nickel, copper, Gemazol Turquoise Blue G, Methylene Blue, and safranin.[17–21] On the other hand, treatment of sugar beet pulp with NaOH, citric acid,[22] and cetyltrimethyl ammonium bromide[23,24] positively affected its pollutant removal potential. Tetra-n-butylammonium bromide (TBAB) was used for the first time for the chemical modification of this biomass and the developed biomaterial was employed for decolorization. Reactive Yellow 2 (RY2) dye was selected in this study as a representative reactive dye. Some kinetic and isotherm models were used to fit the experimental data. Zeta potential values of the biosorbent were measured. IR and SEM–EDX analysis were carried out to characterize the biosorption mechanism. The biosorption performance of the developed biosorbent was also evaluated in real wastewater.

2. Results and discussion

2.1. Effect of pH

The results in Figure 1 indicate that the biosorption of RY2 by both SBP and TBAB–SBP was strongly dependent on pH. The maximum biosorption yields were obtained as 46.41% and 53.73% for SBP and TBAB–SBP, respectively, at pH 2.0. The effect of pH on RY2 biosorption onto both SBP and TBAB–SBP may be attributed to the change in surface charge of the biosorbents with changing pH. According to the zeta potential trend of the biosorbents in Figure 1, the zero point of charges (ZPC) of SBP and TBAB–SBP were +1.9 and –2.79 mV at pH 2.0, respectively. The surface of the biosorbent was positively charged below pH values of ZPC. Therefore, electrostatic interactions between biosorbent surface and negatively charged dye molecules became stronger. Furthermore, the surface charge of TBAB–SBP was more positive than SBP at the investigated pH interval. This could also be an explanation for higher biosorption yield of TBAB–SBP than SBP. When pH $>$ 2.0 the biosorption yields strongly decreased to 9.41% and 7.29%, respectively ($P < 0.05$), and then stayed almost constant ($P > 0.05$). Above pH 5.0, protons transferred from biosorbent decreased the pH of the biosorption medium. On the other hand, at pH $>$ ZPC the biosorption yields of the biosorbents clearly decreased due to the negatively charged surface of the biosorbents. Consequently, pH 2.0 was selected as the optimum value for RY2 biosorption experiments.

2.2. Effect of biosorbent dosage

Figure 2 shows the change in RY2 removal yields onto SBP and TBAB–SBP with biosorbent dosage. RY2 removal yields increased with an increase in the amounts of SBP and TBAB–SBP ($P < 0.05$) and then stayed

constant ($P > 0.05$). This trend may be due to the increased number of binding sites with an increase in the biosorbent dosage. The maximum percentage biosorption of SBP and TBAB–SBP increased from 23.97% to 89.33% and from 26.15% to 96.07%, respectively, with increasing biosorbent amount from 10 to 80 mg. TBAB–SBP also indicated higher RY2 removal percentage than the unmodified form due to its more positive character. Therefore, 80 mg of TBAB–SBP was selected as the appropriate biosorbent in further RY2 biosorption studies.

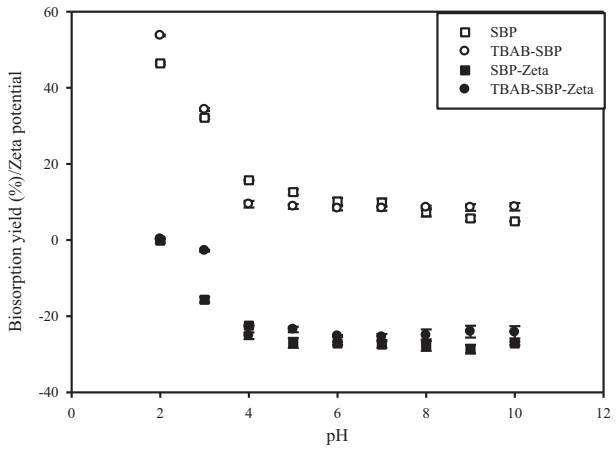

Figure 1. Effect of pH on RY2 biosorption onto SBP and TBAB–SBP and zeta potentials of TBAB–SBP at different pH values.

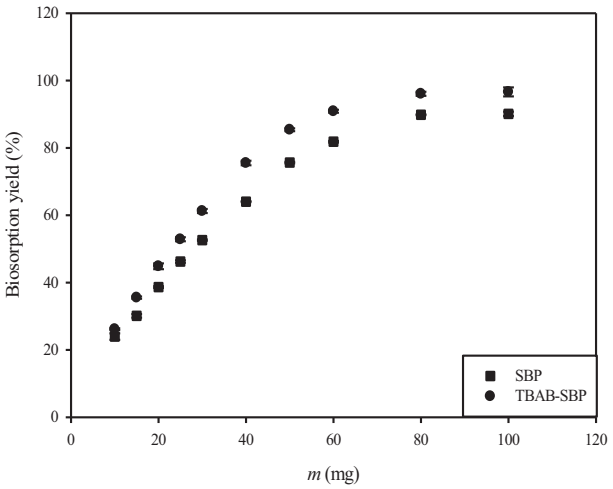

Figure 2. Effect of biosorbent dosage on RY2 biosorption onto SBP and TBAB–SBP in batch system.

2.3. Biosorption kinetics

The effect of contact time on RY2 biosorption onto TBAB–SBP was investigated at three different temperatures (10, 20, and 30 °C) and the obtained data are presented in Figure 3. The biosorption of RY2 onto TBAB–SBP quickly occurred in the first 5 min and then equilibrium was established within 50 min. The temperature did not significantly change the biosorption capacity of TBAB–SBP. This may be an important advantage for the large temperature scale applications of reactive dye biosorption onto TBAB–SBP.

The kinetics of RY2 biosorption onto TBAB–SBP was investigated by the pseudo-first-order and the pseudo-second-order models. The model equations are expressed as follows:

$$\ln(q_e - q_t) = \ln q_e - K_L t \tag{1}$$

$$\frac{t}{q_t} = \frac{1}{k_2 q_e^2} + \frac{1}{q_e} t, \tag{2}$$

where q_t is RY2 biosorption capacity at time t (mg g^{-1}), k_1 and k_2 are the pseudo-first-order (min^{-1}) and the pseudo-second-order rate constants (g mg^{-1} min^{-1}), respectively. The pseudo-second-order kinetic plots and the kinetic parameters for RY2 biosorption onto TBAB–SBP at three different temperatures are presented in Figure 4 and Table 1, respectively. The kinetics of RY2 biosorption onto TBAB–SBP best fitted the pseudo-second-order model and q_e values also agree with the experimental values.

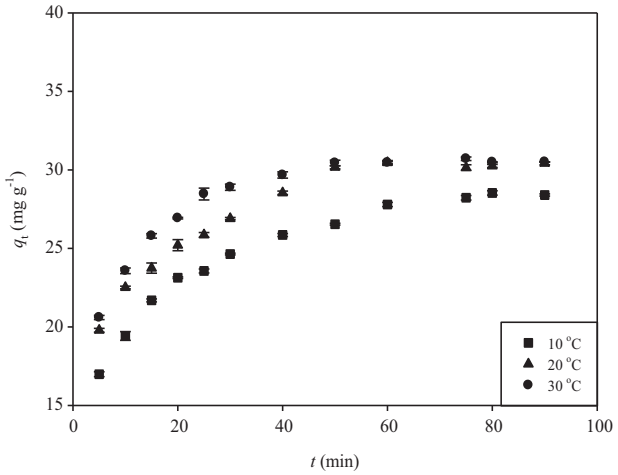

Figure 3. Effect of contact time on RY2 biosorption onto TBAB–SBP at different temperatures.

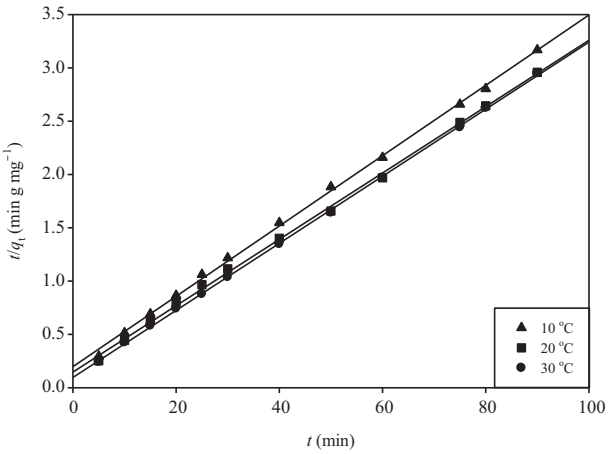

Figure 4. Pseudo-second-order kinetic plots for RY2 biosorption onto TBAB–SBP at different temperatures.

Table 1. Kinetic model parameters for RY2 biosorption onto TBAB–SBP.

Pseudo-second-order				Pseudo-first-order		
t (°C)	k_2 (g mg^{-1} min^{-1})	q_e (mg g^{-1})	R^2	k_1 (min^{-1})	q_e (mg g^{-1})	R^2
10	5.53×10^{-3}	30.30	0.999	4.0×10^{-2}	8.74	0.330
20	6.34×10^{-3}	32.26	0.999	4.8×10^{-2}	8.45	0.326
30	1.03×10^{-2}	31.75	0.999	2.5×10^{-2}	5.39	0.668

2.4. Biosorption isotherms

The isotherm data for the biosorption of RY2 onto TBAB–SBP were analyzed by using nonlinear regression fitting of Freundlich,[25] Langmuir,[26] and D–R [27] isotherm models (Figure 5). The nonlinear equations of these isotherms are represented as follows:

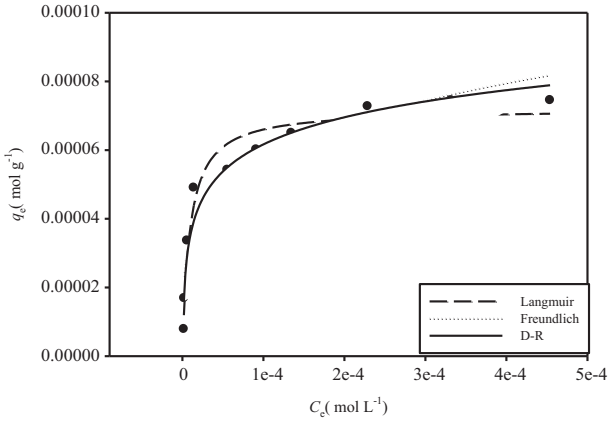

Figure 5. Isotherm plots for RY2 biosorption onto TBAB–SBP.

$$\text{Freundlich: } q_e = K_F C_e^{1/n} \tag{3}$$

$$\text{Langmuir: } q_e = \frac{q_{\max} K_L Ce}{1 + q_{\max} K_L} \tag{4}$$

$$D - R: \ \ln q_e = \ln q_m - \beta\varepsilon^2, \tag{5}$$

where $q_{\max}$ (mol g^{-1}) is the maximum monolayer biosorption capacity, K_L (L mg^{-1}) is the Langmuir constant related to energy of biosorption, K_F (L g^{-1}), and n (dimensionless) are the Freundlich constants showing the biosorption capacity and the intensity, respectively. ε is Polanyi potential determined by $\varepsilon = RT\ln(1+1/C_e)$. β (mol^2 kJ^{-2}) is the D–R isotherm constant indicating the heat of biosorption and used to calculate the biosorption energy (E), which can be calculated from $E = 1/(2\beta)^{1/2}$.

The very close R^2 values of the Langmuir and D–R models in Table 2 indicated that these two models are good fitting isotherms. The maximum monolayer biosorption capacity of TBAB–SBP was 7.20 $\times$ 10^{-5} mol g^{-1}.

Table 2. Isotherm model parameters for RY2 biosorption onto TBAB–SBP.

Langmuir isotherm			
Parameter		t	P
$q_{\max}$ (mol g^{-1})	7.201 $\times$ 10^{-5}	6.328	0.0002
K_L (L mol^{-1})	1.096 $\times$ 10^{6}	5.495	0.0006
R^2: 0.968; S.E.: 0.001; F: 243.617			
Freundlich isotherm			
Parameter		t	P
n	4.398	3.164	0.0133
K_F (L g^{-1})	0.001	6.448	0.0002
R^2: 0.895; S.E.: 8.254 $\times$ 10^{-5}; F: 68.332			
D–R isotherm			
Parameter		t	P
$q_{\max}$ (mol g^{-1})	0.0002	19.623	< 0.0001
$ß$ (mol^2 kJ^{-2})	3.374	13.888	< 0.0001
E(kJ mol^{-1})	0.385		
R^2: 0.960; S.E.: 5.082 $\times$ 10^{-6}; F: 192.867			

A dimensionless constant, R_L, can be used to express the biosorption characteristics and is calculated from the following equation:

$$R_L = \frac{1}{1 + K_L C_o} \tag{6}$$

The R_L value (0.013) in this study indicated the biosorption of RY2 onto TBAB–SBP is favorable.[28] The E value in the D–R isotherm showed that chemisorption plays an important role in the biosorption of RY2 on TBAB–SBP.

2.5. Effect of ionic strength

In order to investigate the influence of ionic strength on decolorization, the biosorption of RY2 on the TBAB–SBP was investigated with different concentrations of KNO_3 at optimum conditions. The results in Figure 6 indicated that an increase in ionic strength leads to a slight decrease in RY2 biosorption. In the absence of

KNO_3, RY2 biosorption yield of TBAB–SBP was 96.07%. However, in the presence of 0.2 M KNO_3 in the biosorption medium, biosorption yield decreased to 86.09%. These results implied that nitrate ions competed with the dye anions for the sorption sites and electrostatic interaction could play a role in the biosorption process.

2.6. Column experiments

In order to evaluate the dynamic flow mode decolorization performance of TBAB–SBP, decolorization experiments were carried out in fixed bed glass columns at various flow rates and bed heights.

TBAB–SBP amount filled into columns was changed between 10 and 200 mg. As is obvious in Figure 7, the biosorption yield of the column increased from 12.63% to 95.54% when the amount of TBAB–SBP was increased from 10 mg to 120 mg. This improvement in the biosorption yield can be attributed to the increased bed height. The increase in bed height increased the mass of TBAB–SBP and surface area available for binding of dye molecules, which led to better performance of the column. Afterwards no further change was observed in the biosorption yield of TBAB–SBP. Therefore, 120 mg of TBAB–SBP was selected as the most efficient biosorbent amount for maximum dye removal.

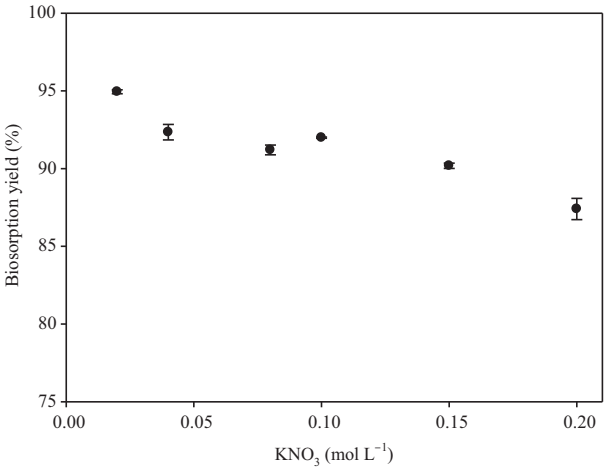

Figure 6. Effect of ionic strength on RY2 biosorption onto TBAB–SBP.

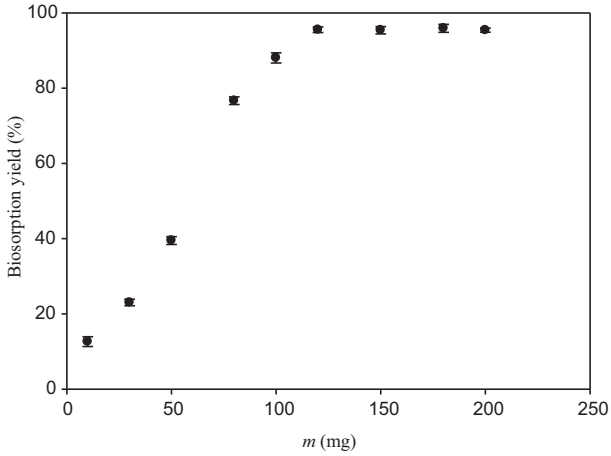

Figure 7. Effect of biosorbent amount on RY2 biosorption onto TBAB–SBP in column system.

The effect of flow rate on the biosorption of RY2 by TBAB–SBP was studied by changing the flow rate from 0.5 to 6 mL min^{-1} and keeping biosorbent amount (120 mg) and initial dye concentration (100 mg L^{-1}) constant. The results are depicted in Figure 8. High biosorption yields ($>96\%$) were recorded at lower flow rates (0.5 and 1.0 mL min^{-1}). When the flow rate was changed from 1.0 to 6.0 mL min^{-1} the dye biosorption yield of TBAB–SBP sharply decreased to 72.11%. This may be explained by the insufficient time for the interaction of RY2 molecules with the functional groups of TBAB–SBP in the column.[29]

2.7. Desorption and regeneration studies

After the biosorption process, biosorbed RY2 dye was desorbed by 0.01 M NaOH at a flow rate of 1.0 mL min^{-1}. The biosorption and desorption cycles were repeated 15 times in order to determine the regeneration potential of TBAB–SBP. The results are shown in Figure 9. It was found that TBAB–SBP maintained its biosorption potential in the first three cycles. A slight decrease was observed in the biosorption potential of TBAB–SBP

after the 4th cycle. At the end of the 15th cycle TBAB–SBP still had 58.35 % biosorption yield. On the other hand, higher than 90% desorption yield was observed. The good regeneration potential of TBAB–SBP clearly indicated that the suggested biosorbent can be a potential and economical candidate for the treatment of reactive dye pollution.

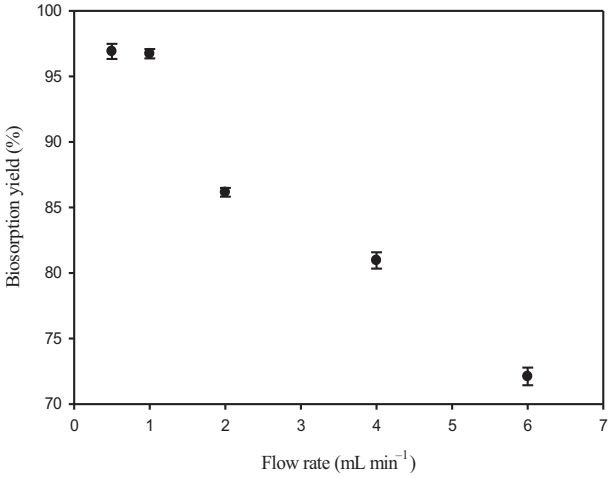

Figure 8. Effect of flow rate on RY2 biosorption onto TBAB–SBP.

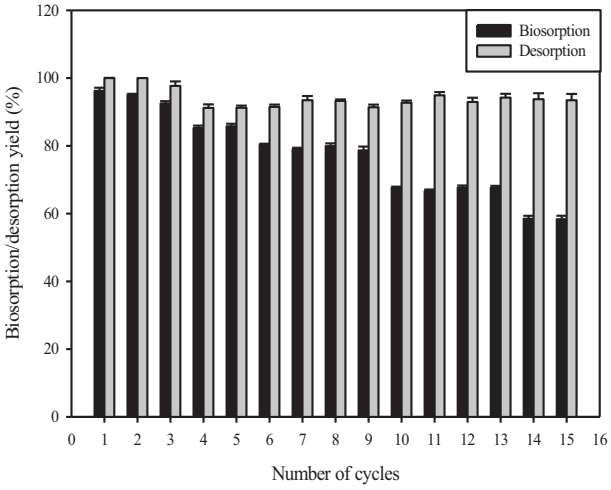

Figure 9. Biosorption/desorption cycles for RY2 biosorption onto TBAB–SBP in column system.

2.8. Biosorbent characterization

The percentages of moisture, volatile compounds, and ash in TBAB–SBP were 8.81%, 91.78%, and 97.30%, respectively. The acidity of the modified biosorbent structure in this study was quantitatively characterized by Boehm titration. The quantities of carboxylic, phenolic, lactonic, and basic groups were 0.45 mmol g^{-1}, 2.26 mmol g^{-1}, 0.63 mmol g^{-1}, and 0.5 mmol g^{-1}, respectively. The high amount of the acidic functional groups indicated the acidic character of the biosorbent surface and improved its anionic dye biosorption efficiency.

The specific surface area and average pore diameter of TBAB–SBP were 2.38 m^2 g^{-1} and 102 Å, respectively.

The functional groups present on the raw biomass surface were determined using IR spectroscopic analysis. The peak positions recorded at 3420, 1744, 1641, 1519, 1437, 1375, 1323, 1248, 1155, 1103, 1059, and 1030 cm^{-1} within the range of 400–4000 cm^{-1} indicated that waste biomass has various possible interaction sites for a pollutant.[23] The effect of chemical modification on the biomass surface and possible dye–biomass interactions were evaluated by IR spectra of TBAB–SBP biomass before and after decolorization (Figure 10). After the modification process, the bands at 1248 (C$-$O stretching) and 1155 cm^{-1} (C$-$O$-$C stretching) in the spectrum of raw biomass shifted to 1254 and 1161 cm^{-1}, respectively. On the other hand, the band at 1518 cm^{-1} (C=C stretching vibration of aromatic skeletal in lignin)[30] in the spectrum of modified biomass disappeared after decolorization. Moreover, intensity decreases were observed in the bands at 1375 (C$-$H bending) and 1254 cm^{-1} (C$-$O$-$C stretching) of dye loaded modified biomass spectrum. This finding indicated that TBAB treatment slightly changed the biosorbent surface and dye molecules were biosorbed by different sites on the modified biosorbent surface.

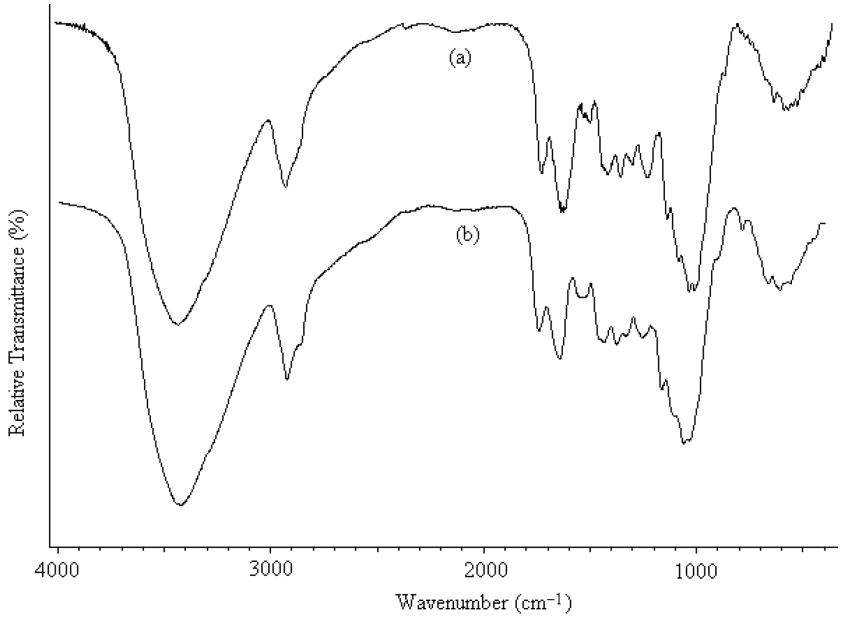

Figure 10. IR spectra of TBAB–SBP and RY2 loaded TBAB–SBP.

In order to reveal the surface features of modified biosorbent after decolorization scanning electron microscopy (SEM) experiments were conducted. SEM micrographs of TBAB–SBP and dye loaded TBAB–SBP at 1500 × magnification are presented in Figure 11. The modified biomaterial possesses a nonuniform and porous structure (Figure 11a). After the biosorption process the relatively rough surface (Figure 11b) of the biosorbent indicated that dye anions are deposited on the modified biosorbent surface like a molecular cloud.

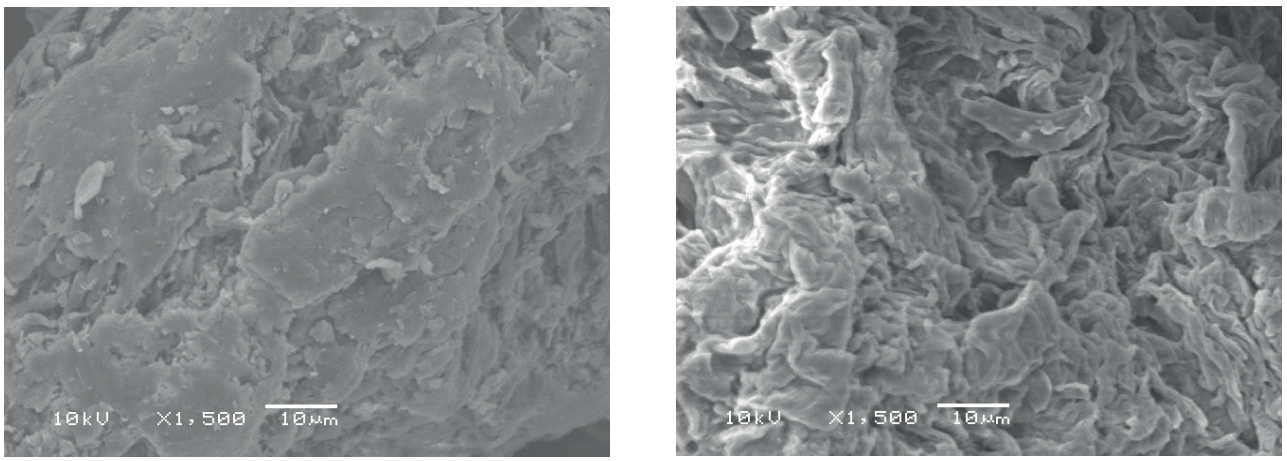

(a) (b)

Figure 11. SEM micrographs of TBAB–SBP (a) and RY2 loaded TBAB–SBP (b).

2.9. Real wastewater treatment

In order to investigate the feasibility of TBAB–SBP implementation on a real treatment application, its RY2 removal performance was investigated with a real wastewater sample. Under optimized conditions, up to 85.93% RY2 dye was extracted from the real wastewater sample and no significant matrix effect was observed.

These findings indicated that TBAB–SBP seems to be a good candidate for the removal of reactive dye from wastewater.

3. Experimental studies

3.1. Biosorbent preparation

Natural sugar beet pulp was treated with 1% (w/v) surfactant (TBAB) solution at 25 °C for 24 h. The modified biosorbent was filtered, washed with deionized water several times, and then dried at 60 °C for 24 h. The modified biosorbent was ground and sieved to 212-μm particle size. It was stored in a glass bottle and used for RY2 biosorption studies.

3.2. Dye solutions

RY2 (C.I.: 18972) was obtained from Aldrich and its chemical structure is included in Figure 12. A stock RY2 solution was used for the preparation of working solutions. pH of the dye solutions was adjusted to required values using HCl and/or NaOH solution.

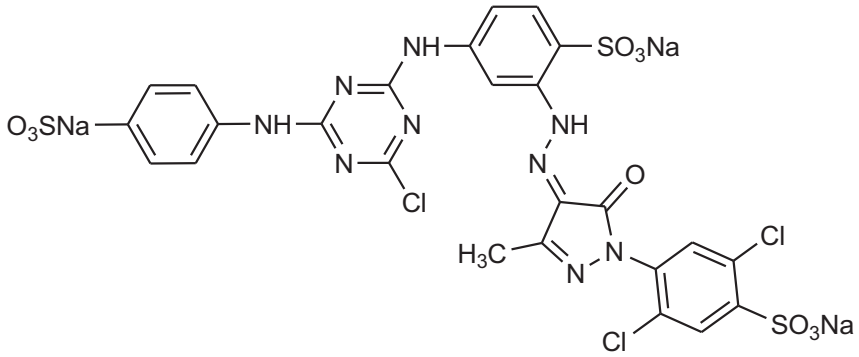

Figure 12. Chemical structure of RY2.

3.3. Biosorption studies

Biosorption experiments in the batch system were carried out on a multipoint magnetic stirrer. First, 25 mg of TBAB–SBP was mixed with 25 mL of dye solutions at different pH values between 2 and 10. Optimum biosorbent dosage was determined by using different amounts of TBAB–SBP between 10 and 100 mg. Contact time was changed between 5 and 90 min at 10, 20, and 30 °C and time-dependent data were used for kinetic evaluation. Next 80 mg of TBAB–SBP was equilibrated with RY2 solutions at various concentrations for isotherm studies. Langmuir, Freundlich, and Dubinin–Radushkevich (D–R) models were used to fit the experimental data. Ionic strength was adjusted between 0.02 M and 0.2 M by adding KNO_3 to the dye solutions.

Continuous flow biosorption experiments were conducted using glass columns with 10-mm internal diameter, and 120 mg of TBAB–SBP was packed between two glass wool layers. RY2 solution was pumped by a peristaltic pump from the bottom of the column.

The concentration of RY2 was analyzed by UV/vis spectrophotometry. The biosorption capacity (q_e) was calculated from the following mass–balance equation:

$$q_e = \frac{V(C_i - C_e)}{m}, \tag{7}$$

where C_i and C_e are the initial and the equilibrium RY2 concentrations (mg L^{-1}), respectively, V is the volume of dye solution (L), and m is the amount of biosorbent used (g).

All the experimental data were presented as the average value of triplicate experiments. SPSS 17 was used to analyze the data and one-way ANOVA was applied to compare average values.

3.4. Instrumentation

The following instrumental methods were used in the biosorption experiments and for the biosorbent characterization:

a) UV spectroscopic analysis: Dye concentrations in the solutions before and after the biosorption procedure were determined by a UV-visible spectrophotometer (Shimadzu UV-2550). For dye analysis 404 nm was selected as the maximum wavelength (λ_{max}).

b) BET surface area analysis: BET surface area, pore size, and total pore volume were measured by Quantachrome Instruments, Autosorb 1 model BET surface area analyzer.

c) Zeta potential measurement: In order to determine the pH-dependent surface charge and the isoelectric point of the modified biosorbent, zeta potentials were measured using a Malvern zetasizer.

d) IR spectral analysis: The surface functional groups of TBAB–SBP were investigated using a Bruker Tensor 27 FTIR spectrophotometer. IR analysis was carried out by KBr disc technique at a wavelength range of 400 and 4000 cm^{-1}.

e) SEM analysis: The biosorbent samples before and after RY2 biosorption were analyzed using a scanning electron microscope (JEOL 560 LV SEM) at 10 keV accelerating voltage and 1500× magnification.

f) Boehm titration method: Acidic and basic functional groups on the surface of biosorbent were determined by a potentiometric titration technique.[31]

4. Conclusion

In the presented study, waste biomass of the sugar production process was successfully modified with TBAB to prepare an effective biosorbent towards an anionic reactive dye. The results of the effect of various operating parameters indicated that the optimum biosorbent amount was 80 mg and the maximum monolayer biosorption capacity was observed at pH 2.0. Biosorption equilibrium was established in 50 min. RY2 biosorption follows the pseudo-second-order kinetic model. Langmuir and D-R isotherm models were more suitable for describing the biosorption of RY2 onto TBAB-SBP. In this examination, we explored an alternative biosorbent for decolorization with the advantages of high biosorption ability, good regeneration, and application potential of TBAB–SBP.

Acknowledgment

The authors are thankful to Eskişehir Osmangazi University (ESOGU) for the financial support. This work was supported by the Commission of Scientific Research Projects of ESOGU (project no: 201219009).

References

1. Vakili, M.; Rafatullah, M.; Salamatinia, B.; Abdullah, A. Z.; Ibrahim, M. H.; Tan, K. B.; Gholami, Z.; Amouzgar, P. *Carbohydr. Polym.* **2014**, *113*, 115-130.
2. Rangabhashiyam, S.; Anu, N.; Selvaraju, N. *J. Environ. Chem. Eng.* **2013**, *1*, 629-641.
3. Robinson, T.; McMullan, G.; Marchant, R.; Nigam, P. *Bioresour. Technol.* **2001**, *77*, 247-255.
4. Fomina, M.; Gadd, G. M. *Bioresour. Technol.* **2014**, *160*, 3-14.
5. Salleh, M. A. M.; Mahmoud, D. K.; Karim, W. A. W. A.; Idris, A. *Desalination* **2011**, *280*, 1-13.
6. Abdolali, A.; Guo, W. S.; Ngo, H. H.; Chen, S. S.; Nguyen, N. C.; Tung, K. L. *Bioresour. Technol.* **2014**, *160*, 57-66.
7. Ömeroğlu Ay, Ç.; Özcan, A. S.; Erdoğan, Y.; Özcan, A. *Colloid Surface B* **2012**, *100*, 197-204.
8. Njoku, V. O. *J. Environ. Chem. Eng.* **2014**, *2*, 881-887.
9. Tunali Akar, S.; Gorgulu, A.; Akar, T.; Celik, S. *Chem. Eng. J.* **2011**, *168*, 125-133.
10. Safa, Y.; Bhatti, H. N. *Chem. Eng. Res. Des.* **2011**, *89*, 2566-2574.
11. Chowdhury, S.; Chakraborty, S.; Saha, P. *Colloid Surface B* **2011**, *84*, 520-527.
12. Noreen, S.; Bhatti, H. N. *J. Ind. Eng. Chem.* **2014**, *20*, 1684-1692.
13. Safa Özcan, A.; Tunali, S.; Akar, T.; Özcan, A. *Desalination* **2009**, *244*, 188-198.
14. Hawari, A.; Khraisheh, M.; Al-Ghouti, M. A. *Chem. Eng. J.* **2014**, *251*, 329-336.
15. Chakraborty, S.; Chowdhury, S.; Das Saha, P. *Carbohydr. Polym.* **2011**, *86*, 1533-1541.
16. Nguyen, T. A. H.; Ngo, H. H.; Guo, W. S.; Zhang, J.; Liang, S.; Lee, D. J.; Nguyen, P. D.; Bui, X. T. *Bioresour. Technol.* **2014**, *169*, 750-762.
17. Reddad, Z.; Gérente, C.; Andrès, Y.; Ralet, M. C.; Thibault, J. F.; Cloirec, P. L. *Carbohydr. Polym.* **2002**, *49*, 23-31.
18. Aksu, Z.; Isoglu, I. A. *Chem. Eng. J.* **2007**, *127*, 177-188.
19. Aksu, Z.; Isoglu, I. A. *J. Hazard. Mater.* **2006**, *137*, 418-430.
20. Vučurović, V. M.; Razmovski, R. N.; Tekić, M. N. *J. Taiwan Inst. Chem. Eng.* **2012**, *43*, 108-111.
21. Malekbala, M. R.; Hosseini, S.; Kazemi Yazdi, S.; Masoudi Soltani, S.; Malekbala, M. R.; *Chem. Eng. Res. Des.* **2012**, *90*, 704-712.
22. Altundogan, H. S.; Arslan, N. E.; Tumen, F. *J. Hazard. Mater.* **2007**, *149*, 432-439.
23. Akar, S. T.; Yilmazer, D.; Celik, S.; Balk, Y. Y.; Akar, T. *Chem. Eng. J.* **2013**, *229*, 257-266.
24. Akar, S. T.; Yilmazer, D.; Celik, S.; Balk, Y. Y.; Akar, T. *Chem. Eng. J.* **2015**, *259*, 286-292.
25. Freundlich, H. Z. *Phys. Chem.-Leipzig* **1906**, *57*, 385-470.
26. Langmuir, I. *J. Am. Chem. Soc.* **1918**, *40*, 1361-1403.
27. Dubinin, M.; Radushkevich, L. *Chem. Zentr.* **1947**, *1*, 875-890.
28. Hall, K. R.; Eagleton, L. C.; Acrivos, A.; Vermeulen, T. *Ind. Eng. Chem. Fundam.* **1966**, *5*, 212-223.
29. Riazi, M.; Keshtkar, A. R.; Moosavian, M. A. *J. Environ. Chem. Eng.* **2016**, *4*, 1890-1898.
30. Pandey, K. K.; Pitman, A. J. *Int. Biodeter. Biodegr.* **2003**, *52*, 151-160.
31. Goertzen, S. L.; Thériault, K. D.; Oickle, A. M.; Tarasuk, A. C.; Andreas, H. A. *Carbon* **2010**, *48*, 1252-1261.